

Tuning Convolutional Spiking Neural Network with Biologically-plausible Reward Propagation

Tielin Zhang, Shuncheng Jia, Xiang Cheng and Bo Xu

Abstract—Spiking Neural Networks (SNNs) contain more biology-realistic structures and biology-inspired learning principles compared with that in standard Artificial Neural Networks (ANNs). SNNs were considered as the third generation of ANNs, powerful on robust computation with a low computational cost. The dynamic neurons in SNNs are non-differential, containing decayed historical states and generating event-based spikes after their states reaching the firing threshold. This dynamic characteristic of SNNs made it hard to be directly trained with standard back propagation (BP) which is considered not biologically plausible. In this paper, a Biologically-plausible Reward Propagation (BRP) algorithm is proposed and applied on a SNN architecture with both spiking-convolution (with both 1D and 2D convolutional kernels) and full-connection layers. Different with standard BP that propagated the error signals from post to pre synaptic neurons layer by layer, the BRP propagated the target labels instead of target errors directly from the output layer to all of the pre hidden layers. This effort was more consistent with the top-down reward-guiding learning in cortical columns of the neocortex. Then synaptic modifications with only local gradient differences were induced with pseudo-BP that might also be replaced with Spike-Timing Dependent Plasticity (STDP). The performance of the proposed BRP-SNN was further verified on spatial (including MNIST and Cifar-10) and temporal (including TIDigits and DvsGesture) tasks. The experimental result showed that the BRP played roles on convergent learning of SNN, reached higher accuracy compared with other state-of-the-art SNN algorithms, and saved more than 50% computational cost compared with that on ANNs. We think the introduction of biologically-plausible learning rules to the training procedure of biologically-realistic SNNs might give us more hints and inspirations towards a better understanding of the intelligent nature of the biological system.

Index Terms—Spiking Neural Network, Biologically-plausible Computing, Reward Propagation, Neuron Dynamics.

I. INTRODUCTION

THE rapid development of deep learning (or Deep Neural Network, DNN) is breaking more research barriers towards a unified solution by easy but efficient end-to-end network learning. DNNs have replaced many traditional machine learning methods on some specific tasks, and the number of these tasks is still increasing [1]. However, during the rapid

expansion process of DNNs, many important and challenging problems were also exposed accordingly, such as adversarial network attacking [2], [3], catastrophic forgetting[4], data-hungry [5], lacking causal inference [6] and low transparency [7]. Some researchers tried to find these answers by taking efforts to the inner-side research of the DNN itself, such as constructing specific network structures, designing more powerful cost functions, or building finer visualization tools so as to open the black box of DNN. These efforts were efficient and also contributed to further development of DNNs [8], [9], [10], however, in this paper, we think that there might be still an alternative and easier approach to achieve these goals especially on robust and efficient computation, by turning into the biological neural networks and then getting efficient-computation inspirations from them towards the human-level robust computation [11], [12], [13], [14], [15], [16], [17], [18].

The Spiking Neural Network (SNN) is considered as the third generation of artificial neural networks (ANNs) [19]. The basic information unit transferred between neurons in SNNs is discrete spikes, containing the precise timing of membrane potential state that reached the firing-threshold. This event-type signal contained not only the information of inner neuronal dynamics but also the historically-accumulated and decayed membrane potential. Spike trains in SNNs, compared to their counterparts, firerates in ANNs, opened a new time coordinate for the better sequential information representation and processing in SNNs. Besides neuron dynamics, biologically-featured learning principles were another key characteristic of SNNs, describing the modification of synaptic weights by local and global plasticity principles. Most of local principles were “unsupervised”, including but not limited as Spike-Timing Dependent Plasticity (STDP)[20], [21], Short-Term Plasticity (STP)[22], Long-term Potentiation (LTP)[23], Long-term Depression (LTD)[24], lateral inhibition[25], [26]. On the meanwhile, global principles are more “supervised”, with fewer number size compared to local principles, and more related to the network functions, e.g., plasticity propagation[27], reward propagation[28], or target propagation[29], [30].

SNNs are different with each other from structures and functions, such as echo state machine[31], liquid state machine[32], feed-forward architecture with dynamic neurons[33], [17], [34], and other SNNs with task-related structures[35], [36], [37], [38], [39]. Until now, some of the tuning methods of SNNs are BP-based (e.g., ReSuMe[40], SpikeProp[41], training with BP and then converting into SNNs[42]) or BP-related (BP through time[43], [44], SuperSpike[45], STDP-type BP[46]). There are still some efforts trying to train SNNs with biologically-plausible plasticity principles (e.g., STDP or

Tielin Zhang was with Institute of Automation, Chinese Academy of Sciences (CASIA), Beijing 100190, China, e-mail: tielin.zhang@ia.ac.cn.

Shuncheng Jia was with CASIA and University of the Chinese Academy of Sciences (UCAS), Beijing 100049, China.

Xiang Cheng was with CASIA and UCAS, Beijing 100049, China.

Bo Xu was with CASIA, UCAS and Center for Excellence in Brain Science and Intelligence Technology, CAS, Shanghai 200031, China, e-mail: xubo@ia.ac.cn.

Tielin Zhang and Shuncheng Jia are co-first authors of this paper. The corresponding authors are Tielin Zhang and Bo Xu.

Manuscript received August 13, 2020; revised XX XX, 2020.

STP-based learning[20], [47], [48], [49], [50], [51], [22], equilibrium learning[52], [53], multi-rule-integration learning[54], [55], curiosity-based learning [56]).

In this paper, we will focus more on the effort of training SNNs with biologically-plausible learning principles instead of directly tuning SNNs with BPs, to get closer to the goal of understanding the brain first and then achieving the human-level artificial intelligence. Hence, a SNN with spiking-convolution layers (containing both 1D and 2D spiking-convolution kernels) and full-connection layers (containing neural dynamics) was constructed and tuned with the proposed Biologically-plausible Reward Propagation (BRP), named as BRP-SNN. The BRP-SNN focused on describing the neuron-level dynamic computation of membrane potential and the network-level rewiring of global synapses. Unlike other tuning methods in SNNs that usually focused more on the local plasticity principles (e.g., STDP and STP) or mixed local and global principles, we used the global BRP only for the simplicity and clarity. After the global reward propagation, synaptic modifications were further induced with only local gradient differences that might also be replaced with STDP or differential Hebb's principle.

Both spatial (including MNIST and Cifar-10) and temporal (including TIDigits and DvsGesture) data sets were used to test the performance of the proposed algorithm on SNNs. High performances were achieved by BRP-SNN (accuracy on test sets, 99.01% for MNIST, 53.11% for Cifar-10, 94.86% for TIDigits, 76.04% for DvsGesture) compared with that by other state-of-the-art (SOTA) SNNs tuned with pure biologically-plausible principles. Furthermore, the BRP-SNN also showed power on low computation cost (saving more than 50% neuron computation). We think this is an alternative effort to achieve biologically efficient learning by tuning biologically-realistic SNN with biologically-plausible global plasticity principles.

II. METHOD

A. Dynamic spiking neurons

The dynamic neurons in SNNs are very different from their counterpart active functions in DNNs. The neurons communicated to each other in different layers of SNNs with the form of discrete event-based spikes, but not continuous firerates in DNNs. DNNs also contain various types of “neurons” (active functions), such as Rectified Linear Unit (ReLU), Sigmoid function, Tanh function. However, they described only the spatial non-linear mapping between input and output signals, instead of temporally wiring them with neuronal dynamics.

$$\begin{cases} C \frac{dV_i(t)}{dt} = g(V_i(t) - V_{rest}) + \sum_{j=1}^N W_{i,j} X_j(t) \\ V_i(t) = V_{reset} \quad \text{if } (V_i(t) = V_{th}, t - t_{spike} > \tau_{ref}) \end{cases} \quad (1)$$

The basic computational units in SNNs are the different types of dynamic neurons[33], for example, Hodgkin-Huxley (H-H) neuron, Leaky Integrated-and-Fire (LIF) neuron, Izhikevich neuron, and spike response neuron (SRM). LIF neuron is one type of the simplest neurons in computational neuroscience describing the dynamics of membrane potential. As shown in Equation (1), the standard LIF neuron dynamically

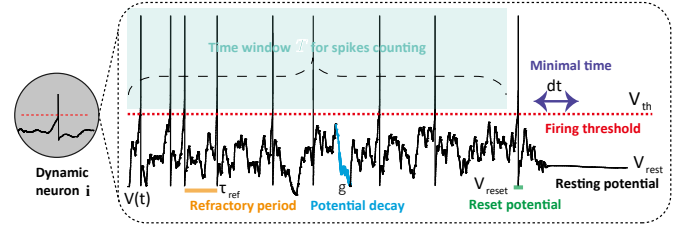


Fig. 1: One example of dynamic LIF neuron in SNN.

updated its membrane potential $V_i(t)$ in a long-range time domain, using hyperparameters such as refractory period τ_{ref} , potential decay of $V_i(t)$ with synaptic conductivity of g , membrane potential reset value V_{reset} when $V_i(t)$ reached the firing threshold V_{th} , resting membrane potential V_{rest} as an attractor of $V_i(t)$ especially when no stimulus input is given. C is the membrane capacitance. dt is the minimal time step for $V_i(t)$ update (usually 1 ms). j is the neuron id of the presynaptic neuron. i is the current neuron id. N is the number of neurons in the current layer. $W_{i,j}$ is the synaptic weight between presynaptic neuron j and current neuron i . t_{spike} is the specific spike time of neuron i . $X_j(t)$ is the neuronal input from presynaptic neuron j . All of the neuronal dynamics will proceed within a time window of T . An example of LIF dynamic neuron in SNN is shown in Fig. 1.

$$\begin{cases} C \frac{dV_i(t)}{dt} = g(V_i(t) - V_{rest})(1 - Spike) + \sum_{j=1}^N W_{i,j} X_j(t) \\ V_i(t) = V_{reset}, Spike = 1 \quad \text{if } (V_i(t) = V_{th}) \\ Spike = 1 \quad \text{if } (t - t_{spike} < \tau_{ref}, t \in (1, T)) \end{cases} \quad (2)$$

Here we added a *Spike* flag into standard LIF neuron in order to block the update of $V_i(t)$ instead of increment of $V_i(t)$ during refractory period. For the dynamic LIF neuron i in Equation (2), the membrane potential $V_i(t)$ is the integration of its historical membrane potential $V_i(t - k)$ ($k \in 1, 2, 3, \dots$) with decay g^k and its current input stimulus $X_j(t)$. As shown in Equation (2), the g (i.e., conductivity) is the decay factor of $V_i(t)$ which is usually designed as a hyper-parameter value smaller than 1 nS. The *Spike* will be generated when the $V_i(t)$ reached the firing threshold V_{th} , and at the same time, the $V_i(t)$ will also be reset as a pre-defined membrane potential V_{reset} . Furthermore, a parameter of refractory time period τ_{ref} is given, during that the neuron i will not fire any spikes even when $V_i(t)$ reached the firing threshold V_{th} . The V_{rest} might also be considered as one attractor of $V_i(t)$ especially when no input $X_i(t)$ was given and no *Spike* generated, where the membrane potential $V_i(t)$ will be dynamically decayed into the V_{rest} . The inner iterative time window T for the calculation of neural dynamics is in a range of 10-100 ms.

B. Spiking-convolution layer with 1D and 2D kernels

The 1D and 2D convolutions have been proved efficiency on temporal and spatial information processing, respectively. The reusability of convolutional kernels (i.e., the sharing of synaptic weights) also contributed to network learning towards the anti-overfitting characteristic of SNN to some extent.

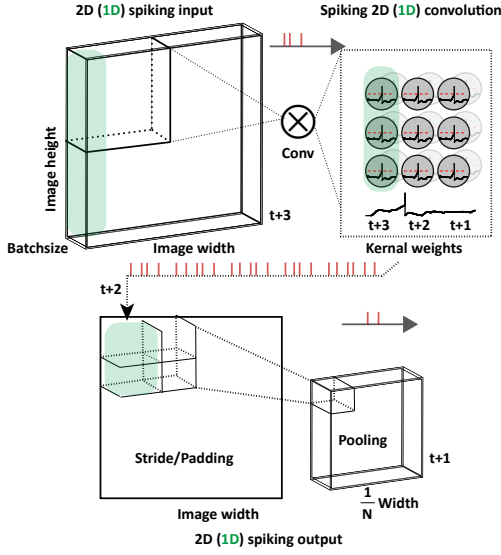


Fig. 2: The 1D and 2D spiking convolution (with pooling)

As shown in Fig. 2, the information in both the input and output of each layer is represented as spike trains. For simplicity, the time clock t that inner the LIF neuron for the membrane potential update is designed as the same with the outside neuron clock t that used for the signal propagation from pre to post layers. This means the time range of information propagation within and outside of neuron are all T for the ease of computation. The convolutional layer received 2D (or 1D) spiking input with height and weight dimensions (or only height dimension for 1D input, a green bar, Fig. 2), and then made the convolution with 2D (or 1D, LIFs in the green bar, Fig. 2) kernels. All of the neurons in kernels were designed as dynamic neurons containing spikes that encoded the event-based signals with learning time t going by (until T). Then spikes after convolution further proceeded with pooling for dimension reduction.

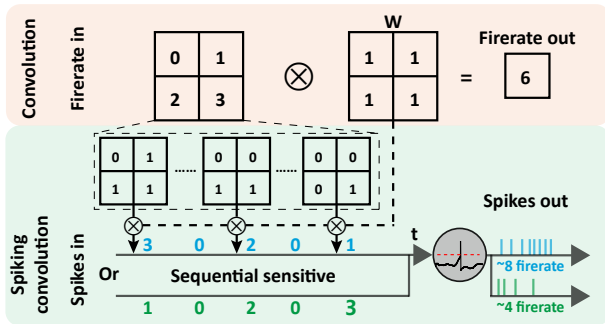


Fig. 3: Schematic diagram depicting the procedures of the standard convolution in DNN and the spiking convolution in SNN.

The convolutional processing in SNNs is different from that in traditional DNNs. For a clearer description of the differences between traditional and spiking convolutions, a schematic diagram of two types of convolutions was described and shown in Fig. 3. In SNNs, the convolutional layer receives

sequential spike inputs and then generate output spikes affected by the membrane potential decay and the historical signal integration. The decay of membrane potential will make the LIF neuron harder to fire so that output fewer spikes, while on the contrary, the historical integration of membrane integration will make LIF easier to fire so that output more spikes. These two dynamical parts in LIF will contribute to the temporal information processing of SNN at the micro-scale neuron level.

As an example shown in Fig. 3, the same amount of firerates were given to both SNNs and ANNs. SNNs were sensitive to input firerates that contained temporal spikes, hence producing different spikes (firerates) according to different input-spike sequences. On the contrary, ANNs only output the same firerates ignoring the temporal differences of input signals. This sequence-related dynamics of LIF neuron in SNNs will contribute to the temporal signal learning compared to standard artificial active functions in ANNs.

C. The architecture of BRP-SNN

The whole BRP-SNN architecture is shown in Fig. 4, where input spike trains were generated and encoded from raw signal input, which might be the raw 1D auditory signal or 2D image signal. For 1D and 2D signals without spikes (e.g., TIDigits and Cifar-10), the raw input signals $I_{raw}(t)$ were randomly sampled as the sequential spike train $I_{spikes}(t)$ first, and then propagated into the following convolutional, pooling and full-connection layers. For signals with natural spikes, such as the 3D dynamic-vision-sensor (DVS) video signals (e.g., DvsGesture), the raw signals were already well encoded with 0 or 1 event-type symbols which might be considered as spikes directly. Hence the additional spike encoding procedure was not necessary. The spike generator is shown in Equation (3). I_{rd} is a 0-1 random variable generator with decay factor α , where $I_{rd}(\alpha) = I_{rd} * \alpha$. T is the time window of the network clock that is set the same as the inner clock of LIF neurons.

$$I_{spikes}(t) = \sum_{i=1}^T \delta(t - t_i) (I_{raw}(t) < I_{rd}(\alpha)) \quad (3)$$

The spiking-convolution and pooling layers were also constructed for the spatial feature detection, and then feedforward full-connection layers were constructed for the further network classification. Spike trains of different hidden layers in SNNs would be summed as firerates first after the whole time window T , then combined with propagated label-reward signals for the local synaptic modification.

D. Tuning SNN with global BRP

Feed-forward and feed-back propagations were usually interleaved together for convergence learning of SNNs. The feed-back propagation was also described as the top-down refinement of the network structure (e.g., synaptic weights) with targets (e.g., error cost functions in BP) or network states first (revised or pseudo-BPs) and then consolidated into synaptic weights[12]. However, these BPs were considered not

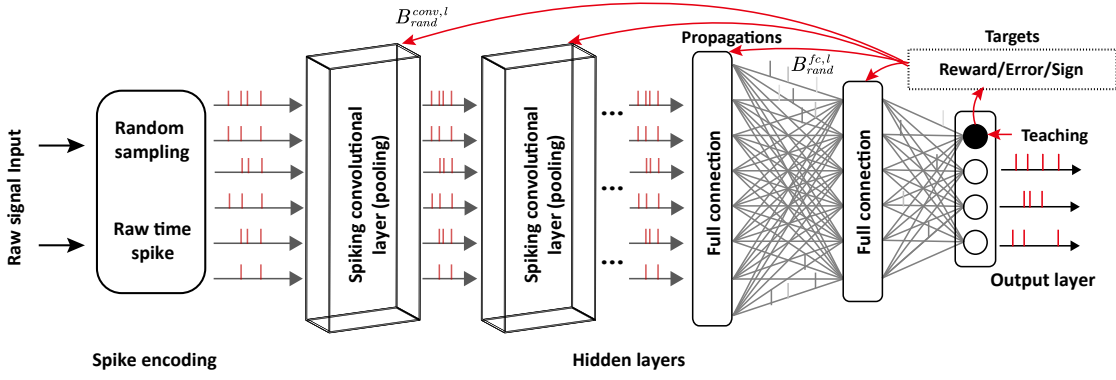


Fig. 4: The architecture of BRP-SNN.

biologically plausible for their layer-by-layer error backpropagation.

In the biological system, the signal might be backpropagated within inner neurons or only within neighborhood layers [57], [58], [59], [12], [60]. Long-range propagation is usually with the form of reward propagation from neurons in the brain region for higher cognitive functions directly to target neurons in the brain region for primary cognitive functions [12]. The idea of a direct random target propagation algorithm [29] is very fit for these biological constraints. Hence here we selected it as the underlying bone architecture of BRP and made a further refinement of it with neuron dynamics, spiking convolutions, and reward propagations.

$$TP_{BRP} = Label_{spikes}(t) \quad (4)$$

The proposed reward propagation BRP is shown in Equation (4), describing the target label (the one-shot $Label_{spikes}(t)$ during T) as the reward to directly propagate to all of pre hidden layers.

$$TP_{err} = y(t) - \bar{y}(t) \quad (5)$$

Different with TP_{BRP} , another two candidates TP_{err} and TP_{sign} were also constructed. TP_{err} described the differences between output signals and teaching signals for propagation, as shown in Equation (5). $\bar{y}(t)$ is the mean firerates of the teaching signals ($Label_{spikes}(t)$). $y(t)$ is the mean summation of output spike trains of SNN ($O_{spikes}(t)$), as shown in Equation (6). The spikes in time window T were summed together as fire rate $y(t)$ only at the end of T ,

$$\begin{cases} y(t) = \frac{1}{T} \sum_{t=1}^T O_{spikes}(t) \\ \bar{y}(t) = \frac{1}{T} \sum_{t=1}^T Label_{spikes}(t) \end{cases} \quad (6)$$

TP_{sign} described the sign of positive and negative errors for propagation. As shown in Equation (7), the detailed error signal is not necessary, and only the sign of the error was used for the propagation. This effort propagated only positive (“+”) and negative (“-”) signals to hidden layers. This type of signal seems like a reward. However, this calculation of sign was with the premise that detailed errors had to got first and then quantitatively normalized as signs of errors. Hence it still

needed both $y(t)$ and $\bar{y}(t)$, the same with TP_{err} , instead of the pure reward definition that related only with the functional goal of the network.

$$TP_{sign} = sign(y(t) - \bar{y}(t)) \quad (7)$$

Different types of TPs will directly propagate to all of the hidden layers, including spiking-convolution layers and full-connection layers. The additional B_{rand} will be given as a randomly generated matrix during the network initialization, which played roles on the different-dimensional matrix conversion from the output layer to pre each hidden layer. Notice that the global propagation might only propagate signal and affect the neuron states (e.g., membrane potential) instead of the synaptic weights. Hence, the synaptic modification for the learned knowledge will be further processed in the next-step local synaptic weight consolidation.

E. The local synaptic weight consolidation

The BRP will propagate back directly into different hidden layers of SNN at time t . This effort will influence the current network states, and at the same time, give SNN a desired target state for the next-step learning at time $t + 1$. The tuning of synaptic weights in SNNs may updated based on the difference of the local propagated neural state $B_{rand}^{conv,l} * TP_{BRP}(t)$ and the current neural states $h^{conv,l}$.

$$\Delta W_{i,j}^{conv,l} = -\eta^{conv} (B_{rand}^{conv,l} * TP_{BRP}(t) - h^{conv,l}) \quad (8)$$

$$\Delta W_{i,j}^{fc,l} = -\eta^{fc} (B_{rand}^{fc,l} * TP_{BRP}(t) - h^{fc,l}) \quad (9)$$

As shown in Equation (8) and Equation (9). The $B_{rand}^{conv,l}$ and $B_{rand}^{fc,l}$ were random generated matrixs for each hidden layer l before network learning and would not be further updated during learning. $\Delta W_{i,j}^{conv,l}$ is the synaptic weight in convolutional layer l from the presynaptic neuron j to the post synaptic neuron i . $\Delta W_{i,j}^{fc,l}$ is the synaptic weight in full-connection layer l from the presynaptic neuron j to the post synaptic neuron i . η^{conv} and η^{fc} are learning rates. $h^{conv,l}$ and $h^{fc,l}$ are neuron states in current layer l .

F. The pseudo gradient approximation

The dynamic LIF neuron in SNN is non-differential, which is hard to propagate the gradient for the further calculation of the gradient from global BRP to local weight consolidation. Traditional local tuning of SNNs used STDP or differential Hebb's principle for the locally synaptic modification according to the state difference of pre and post synaptic neurons [49], [20], [51]. Unlike that, here we give an additional pseudo gradient approximation of LIF neurons to tuning SNNs within the Pytorch architecture [61]. The pseudo gradient converted the non-differential procedure of neuron firing (the membrane potential $V_i(t)$ reached the firing threshold V_{th} and set as V_{reset}) as a specific pseudo gradient, as shown in Equation (10), where traditional $\Delta V_i(t)$ is infinite when $V_i(t) = V_{th}$ and here we set $\Delta V_i(t) = 1$ during the back propagation, as an approximately finite pseudo gradient of $\Delta V_i(t)$.

$$\Delta V_i(t) = V_i(t+1) - V_i(t) = 1 \quad \text{if}(V_i(t) = V_{th}) \quad (10)$$

G. The algorithm complexity analysis

One of the most advantages of using biologically-plausible algorithms to tune K-layer SNNs is the lower algorithm complexity. As shown in Table I, for the pure STDP, an update of synaptic weight was induced directly during the feedforward information propagation. Hence the algorithm complexity is $O(nK + mK)$, where n and m are computational costs of one-step feedforward and one-step local plasticity propagation, respectively.

TABLE I: Algorithm complexity for tuning K-layer SNNs

Strategy	Complexity
Pseudo BP	$O(nK + m(m+1)K)$
BRP	$O(nK + (m+1)K)$
Pure STDP	$O(nK + mK)$

BRP also has the feedforward procedure $O(nK)$, but parallelly propagating reward from the output layer to all hidden layers with an additional one-step matrix conversion ($B_{rand}^{conv,l}$ and $B_{rand}^{fc,l}$), hence the algorithm complexity is $O(nK + (m+1)K)$. For pseudo BP, besides the $O(nK)$ feedforward cost, it also contains the multi-step back propagations step by step with differential chain rule, hence cost during BP is $O(nK + m(m+1)K)$.

H. The learning procedure of BRP-SNN architecture

The detailed learning procedure of BRP-SNN is shown in Algorithm 1

III. EXPERIMENTS

A. The spatial data sets

The MNIST [62] and Cifar-10 [63] are selected as the two examples of spatial data sets. The MNIST contains 7,000 28x28 1-channel gray hand-written digit-number images from 0-9, in which 60,000 samples are selected out as training samples, and remained 10,000 samples are used for testing. The Cifar-10 contains 60,000 32x32 3-channel color images

Algorithm 1 The learning procedure of BRP-SNN.

1. Start network initialization: Pack raw data set as input to SNN with or without spikes generation by random sampling; Initialize all of hyper parameters, related with dynamic neurons C , g , dt , V_{rest} , $W_{i,j}$, V_{reset} , τ_{ref} , and other related parameters of network, e.g., kernel size, kernel numbers, number of hidden layers and neurons, learning rates η^{conv} and η^{fc} , propagation matrixs of $B_{rand}^{conv,l}$ and $B_{rand}^{fc,l}$ in each layer l , time window T ;
2. Start Training procedure:
 - (1). Load training samples;
 - (2). Feed-forward information propagation of I_{spikes} from spiking-convolution to full-connection layers;
 - (3). Iteratively increase the network clock t and output O_{spikes} until t reached the time window T ;
 - (4). Calculate the fire rate of network $y(t)$ until the end of T ;
 - (5). Propagation of TP_{BRP} , TP_{err} or TP_{sign} to spiking-convolution and full-connection layers based on Equation (4-7);
 - (6). Update neuron states in each layer with global BRP;
 - (7). Update synaptic weights with local state differences (pseudo gradient) based on Equation (8-10);
 - (8). Iteratively train BRP-SNN from Step (2) to Step (7) until convergence; save the tuned synaptic weights in all layers.
3. Start testing procedure:
 - (1). Load test samples;
 - (2). Test the performance of BRP-SNN with feedforward propagation based on saved synaptic weights in each layer.
 - (3). Output the neuron ids with maximum firerate $y(t)$ in time window T as the target class; calculate the accuracy in the whole test data set without cross-validation.
4. End SNN learning.

covering 10 classes, in which 50,000 for training and 10,000 for test. The samples in both of them are static 2D images; hence a further procedure of spike generation is needed.

B. The temporal data sets

TIDigits [64] and DvsGesture [65] are selected out as the two examples of temporal data sets. TIDigits contains 4,144 (20K HZ and around 1 second for each sample) spoken digits from 0-9. DvsGesture data set contains 1,464 128x128x1800 gesture samples (with event-based 1,800-frame DVS video, and we low-sampled them as 32x32 size and 100 frames for the ease of computation) covering 11 gesture types. These two data sets are challenging on the temporal information processing, for example, TIDigits contains sequential pronounce of spoken numbers, and DvsGesture contains sequential videos different from contents of clockwise and counterclockwise arm rotations. Signals in TIDigits are continuous; hence a further procedure of spike generation is needed. Signals from the DvsGesture data set were recorded from DVS camera; hence might be considered as natural spikes without an additional procedure of spike conversion.

C. The configuration of hyper parameters

Parameters of BRP-SNN for different tasks are different with each other after a little refinement for reaching higher performances. The refined network topologies are shown in Table II, including the number of spiking-convolution layers and the number of full-connection layers. η^{conv} and η^{fc} were $1e-4$. For LIF neurons, $C = 1 \text{ uF/cm}^2$, $g = 0.2 \text{ nS}$, $\tau_{ref} = 1 \text{ ms}$, $T = 10\text{-}100 \text{ ms}$, $V_{th} = 0.5 \text{ mV}$, $V_{reset} = 0 \text{ mV}$. The local pseudo gradient computation used MSE loss and Adam optimizer. Batch size for all tasks was normalized as 50.

TABLE II: BRP-SNN parameters for different tasks

Tasks	Topology	Parameters
MNIST	Cov5*5x28-28-FC1000-FC10	$I_{rd}(\alpha)=1$, $\eta=1e-4$
Cifar-10	Cov5*5x32-S2-FC1000-FC10	$I_{rd}(\alpha)=1$, $\eta=1e-4$
TIDigits	Cov1*3x100-S1-FC1000-FC10	$I_{rd}(\alpha)=0.1$, $\eta=1e-4$
DvsGesture	Cov5*5x32-S2-FC1000-FC10	$I_{rd}(\alpha)=1$, $\eta=1e-4$

D. BRP contributed to convergence learning of SNNs

The learning convergence is usually the premise of next-step efficient learning in all types of networks. As shown in Fig. 5, three types of biologically-plausible propagations were tested during the learning of the four tasks, including the proposed BRP in Equation (4), the error propagation in Equation (5), and sparse error sign propagation in Equation (7). The time window T for these two data sets are predefined as $T=20$ (for MNIST, Cifar10, and TIDigits data sets) and $T=30$ (for DvsGesture data set) for the consideration of better performances. The learning results on both training and testing sets showed that all three biologically-plausible propagations were convergent on four tasks.

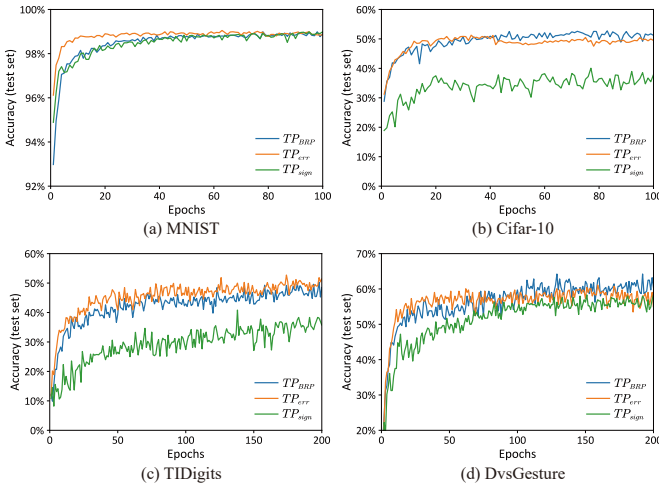


Fig. 5: Network convergence with different TPs on SNNs

For the MNIST data set, the SNN using TP_{BRP} was convergent on the test set with the increasement of training epochs from 0 to 100. SNNs using TP_{BRP} also got a convergence rate that was higher than that in TP_{sign} but lower than that in TP_{err} . The final accuracy for TP_{BRP} , TP_{err} and TP_{sign} reached 98.89%, 98.85% and 98.99%, respectively.

Similar with that for MNIST, for Cifar-10 and TIDigits data sets, the SNNs using TP_{BRP} were also convergent and

got convergence rates higher than that using TP_{sign} and comparable to that using TP_{err} . The final accuracy for SNNs using (TP_{BRP} , TP_{err} and TP_{sign}) reached (51.21%, 49.48% and 37.85%) on Cifar-10 and (48.55%, 51.45% and 35.69%) on TIDigits, respectively.

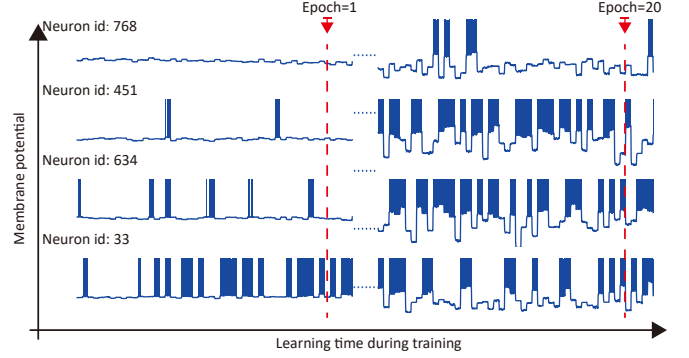


Fig. 6: Membrane potentials with spikes during the training of BRP-SNN

For the DvsGesture data set, the TP_{BRP} outperformed both TP_{err} and TP_{sign} on testing convergence rate, by reaching both the higher accuracy and higher convergence rate. The final accuracy for TP_{BRP} , TP_{err} and TP_{sign} reached 60.42%, 54.86% and 58.33%, respectively.

Furthermore, membrane potentials with spikes were also plotted for some neurons in full-connection layers of BRP-SNN. The ids of neurons were randomly selected, as shown in Fig. 6. The neural states were dynamically changed during the learning procedure of BRP-SNN from epoch 1 to epoch 20, and shown with a better information representation (with more frequent and more stable neuron firing). For achieving higher performances, additional experiments were also designed with larger epochs. Finally, the accuracy of SNNs using BRP reached 99.01% (MNIST) and 52.56% (Cifar-10) after 400 epochs, and reached 65.68% (TIDigits) and 64.93% (DvsGesture) after 10,000 epochs. These high performance of BRP on four benchmarks showed the network efficiency on both accuracy and convergency.

E. BRP reached comparable performance with pseudo-BP

The inner-neuron time window T described the encoding ability of neuronal dynamics, especially for temporal information. As shown in Fig. 7(a,b), for spatial data sets, accuracies of SNNs trained with BRP for different T (from 10 to 30) are similar (around $98.99 \pm 0.01\%$ for MNIST and around $52.65 \pm 0.61\%$ for Cifar-10). One of the main reasons for this result was that the spatial data didn't contain any temporal information, and the temporal spike trains used for classification were generated from the random spike generator. This hypothesis was further verified by the test of temporal data sets with SNNs using different T in Fig. 7(c,d), where accuracies of SNNs on temporal tasks (from 62.46% to 71.14% on TIDigits, from 69.10% to 76.04% on DvsGesture) showed a linearly-increase relationship with the size of time window T (from 10 to 30 on TIDigits and from 30-90 on DvsGesture).

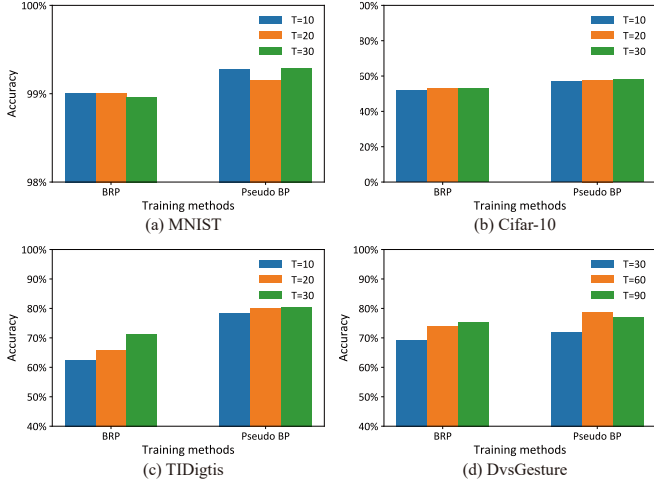


Fig. 7: Accuracy comparisons of spatial and temporal tasks between BRP and BP for different T

Furthermore, the performance of SNNs using BRP reached a comparable performance with standard pseudo-BP. The accuracies for SNNs using BRP and using BP reached, (99.01% and 99.29%) on MNIST, (53.11% and 57.88%) on Cifar-10, (71.14% and 80.31% with 1D kernels, 94.86% and 95.10% with 2D kernels) on TIDigits, (76.04% and 78.21%) on DvsGesture, respectively.

In conclusion, we found that when tuning SNN with BRP, the differences of accuracy compared with that tuned with best BP, were no more than 0.28%, 4.77%, 0.24%, and 2.17%, on MNIST, Cifar-10, TIDigits, and DvsGesture, respectively.

F. The comparison of BRP-SNN with other SOTA methods

We further tested the performance of our BRP-SNN with other SOTA algorithms, including spike-based and rate-based SNNs. Some non-biologically-plausible algorithms were also listed for a better comparison. As shown in Table III, for the MNIST task, the best accuracy of SNN was trained with BP, where signals were represented with firerate (99.1%). Our BRP-SNN algorithm reached the accuracy of 99.01% with spike signals and tuned with biologically-plausible BRP, which was higher than other SNNs tuned with STDs.

For the Cifar-10 data set, we only made a further comparison with [56] for its biologically-plausible learning principles (with curiosity and STDP). Our BRP-SNN reached 53.11% accuracy, which is higher than the curiosity-based SNN (52.85%).

For the TIDigits data set, we got 71.14% and 94.86% accuracies on 1D and 2D convolutional SNNs, respectively. For the liquid state machine SNN, the accuracy only reached 92.30%. For the integration of ANN (e.g., SOM) and SNN, the accuracy was higher than us and reached 97.40%. This effort showed the power of the hybrid architecture by the integration of both SNNs and ANNs.

For the DvsGesture data set, our 2D-convolutional SNN reached 76.04% accuracy, which, as far as we know, was the first time to use a biologically-plausible learning principle to

train the spike-based SNNs without any preprocessing and cooperation with other methods. These results showed the efficiency of proposed BRP-SNN.

G. Low computation cost of BRP-SNN with silent neurons

In ANNs, some signals with minimal values were surprisingly important, for example, the BP gradient values that smaller than $1e-6$ (still played roles on synaptic modification), or the firerates in output neurons for the next-step target class judgment based on not absolute but relative values compared with firerates of other output neurons. Hence, ANNs have to take more computational resources to deal with these special situations.

In SNNs, the basic unit of signals was a discontinuous spike. The neurons that hadn't received any spikes, or received but still not firing (without enough input spikes to make the membrane potential reach the firing threshold), could be considered as the silent neurons. These silent neurons will take nearly no computational cost on specially designed neuromorphic chips [69]. Hence, the number of these silent neurons in different layers of SNNs during the network learning could be a good indicator for calculating computational cost with the combination of the algorithm complexity, under the condition that these SNNs reached the same level of accuracy.

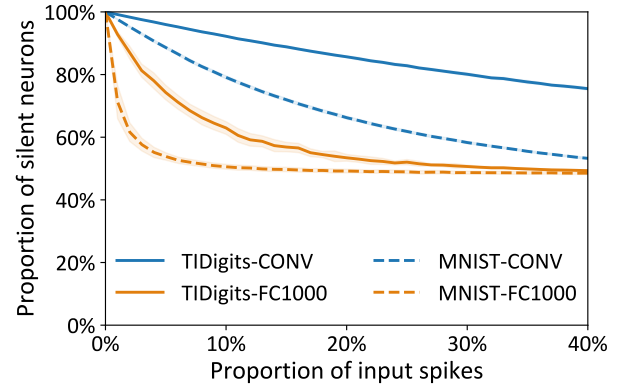


Fig. 8: The proportions of silent neurons in different hidden layers of SNNs (trained on MNIST and TIDigits data sets), with the proportional increasement of input spikes in the first layer

As shown in Fig. 8, MNIST, and TIDigits were selected out as two representatives of spatial and temporal tasks, respectively. The proportion values of silent neurons were all decreased with the proportional increment of input spikes (from 0% to 40%), in different hidden layers of SNNs trained with MNIST and TIDigits. For spiking-convolution (CONV) and full-connection (FC1000 with 1000 hidden neurons) layers, more than half of neurons were silent, and these proportion values were reduced when a more significant proportion value of input spikes was given. When the proportion of input spikes reached 40%, the proportion values of silent neurons reached 53.26% (CONV) and 48.52% (FC1000) on spatial MNIST data set, that were much smaller (means more computational cost) than that on temporal TIDigits data set, reached 75.50% (CONV) and 49.32% (FC1000).

TABLE III: The performance comparisons of the proposed BRP-SNN with other SOTA algorithms on four tasks

Task	Architecture	Training Type	Learning Rule	Performance
MNIST	Three-layer SNN [51]	Spike-based	Equilibrium learning + STDP	98.52%
	Three-layer SNN [53]	Spike-based	Balanced tuning +STDP	98.64%
	Convolutional SNN [66]	Rate-based	Backpropagation	99.1%
	2D-convolutional SNN (Ours)	Spike-based	BRP	99.01%
Cifar-10	Three-layer SNN[56]	Spike-based	Curiosity+STDP	52.85%
	2D-Convolutional SNN (Ours)	Spike-based	BRP	53.11%
TIDigits	SOM-SNN [67]	Rate+Spike	SOM+BP	97.40%
	Liquid State Machine [68]	Spike-based	BP	92.30%
	1D-convolutional SNN (Ours)	Spike-based	BRP	71.14%
	2D-convolutional SNN (Ours)	Spike-based	BRP	94.86%
DvsGesture	2D-convolutional SNN (Ours)	Spike-based	BRP	76.04%

Hence, SNNs, to this extent, at least saved more than 50% computational cost, on the perspective of a relatively much smaller number of computing neurons (more silent neurons) than in ANNs. In addition, a lower computational cost might be achieved more likely on temporal tasks compared with that on spatial tasks.

IV. CONCLUSION

During the evolution of millions of years, the biological brain is increasingly more efficient in the representation and processing of complex signals, with spikes, delicately designed network structures, and efficient biologically-plausible plasticity principles. SNNs are from the inspiration of biological networks, containing discontinuous spikes instead of continuous firerates for information propagation. These seem-simple spikes are not trivial but have played essential roles in the sparse- and event-coding of signals. They also reflected the complex inner computation of neuronal dynamics and the balance computation between higher accuracy and lower computational cost. SNNs also contained various types of plasticity principles, including local plasticity principles (e.g., STDP, STP, Hebb, lateral inhibition) and global plasticity principles (e.g., dopamine-like reward that was propagated directly along with top-down connections from reward neurons to target neurons, without any multi-step routing).

In this paper, we focused on both spikes from neuronal dynamics and biologically-plausible learning principles on the good tuning of SNNs, not for the highest accuracy, but an alternative effort to better understand a possible efficient tuning strategy in the real biological brain. Inspired from the direct reward signal propagation in the brain, we designed a SNN using Biologically-plausible Reward Propagation (BRP-SNN) to directly propagate the right label index (with the form of spikes) to target neurons. Spiking-convolution and full-connection layers with dynamic LIF neurons were constructed for the BRP-SNN and verified on four benchmark data sets, including spatial data sets (MNIST and Cifar-10), and also temporal data sets (TIDigits and DvsGesture). The BRP-SNN got comparable performances with that tuned with SOTA pseudo-BP under the same SNN architectures. They reached testing accuracy with 99.01% for MNIST, 53.11% for Cifar-10, 94.86% for TIDigits, and 76.04% for DvsGesture, respectively. A further computation-efficiency analysis was given, and the result showed that the BRP-SNN saved at least 50% computational cost on both full-connection layers and spiking-convolution layers compared with that in standard ANNs.

The standard BP in ANNs back propagates error signals from the final output neurons to pre neurons layer by layer, which is not only non-biologically-plausible but also not-energy-efficient. We think the deeper research on biologically-plausible plasticities (e.g., BRP or other not integrated into this paper but important local plasticities such as STDP and STP) applied on the biologically-realistic networks, would someday finally replace BP, toward human-level robust computation, energy-efficient learning, or artificial general intelligence that the community of artificial intelligence is facing but still not resolved. We think this research will also give us more hints on the better understanding of the intelligent nature of the biological system, or promote a better study development of global neural plasticity on neural biology.

ACKNOWLEDGMENT

This paper is supported by the National Natural Science Foundation of China (61806195), the Strategic Priority Research Program of the Chinese Academy of Sciences (XDBS01070000), and the Beijing Brain Science Project (Z181100001518006). The source code of BRP-SNN will be released after the paper's acceptance. The source code link on the github page is <https://github.com/thomasaimondy/BRP-SNN>.

REFERENCES

- [1] Y. LeCun, Y. Bengio, and G. Hinton, "Deep learning," *Nature*, vol. 521, no. 7553, pp. 436–444, 2015.
- [2] X. Chen, Y. Duan, R. Houthoofd, J. Schulman, I. Sutskever, and P. Abbeel, "Infogan: interpretable representation learning by information maximizing generative adversarial nets," in *neural information processing systems*, 2016, Conference Proceedings, pp. 2180–2188.
- [3] A. Nguyen, J. Yosinski, and J. Clune, "Deep neural networks are easily fooled: High confidence predictions for unrecognizable images," in *computer vision and pattern recognition*, 2015, Conference Proceedings, pp. 427–436.
- [4] J. Kirkpatrick, R. Pascanu, N. C. Rabinowitz, J. Veness, G. Desjardins, A. A. Rusu, K. Milan, J. Quan, T. Ramalho, and A. Grabszabarska, "Overcoming catastrophic forgetting in neural networks," *Proceedings of the National Academy of Sciences of the United States of America*, vol. 114, no. 13, pp. 3521–3526, 2017.
- [5] B. M. Lake, R. Salakhutdinov, and J. B. Tenenbaum, "Human-level concept learning through probabilistic program induction," *Science*, vol. 350, no. 6266, pp. 1332–1338, 2015.
- [6] B. M. Lake, T. Ullman, J. B. Tenenbaum, and S. J. Gershman, "Building machines that learn and think like people," *Behavioral and Brain Sciences*, vol. 40, pp. 1–101, 2017.
- [7] A. Mahendran and A. Vedaldi, "Visualizing deep convolutional neural networks using natural pre-images," *International Journal of Computer Vision*, vol. 120, no. 3, pp. 233–255, 2016.

- [8] S. Sabour, N. Frosst, and G. E. Hinton, "Dynamic routing between capsules," in *Advances in Neural Information Processing Systems*, 2017, Conference Proceedings, pp. 3859–3869.
- [9] B. Scellier and Y. Bengio, "Equilibrium propagation: Bridging the gap between energy-based models and backpropagation," *arXiv preprint arXiv:1602.05179*, 2016.
- [10] G. Zeng, Y. Chen, B. Cui, and S. Yu, "Continual learning of context-dependent processing in neural networks," *Nature Machine Intelligence*, 2019.
- [11] D. Hassabis, D. Kumaran, C. Summerfield, and M. Botvinick, "Neuroscience-inspired artificial intelligence," *Neuron*, vol. 95, no. 2, pp. 245–258, 2017.
- [12] T. P. Lillicrap, A. Santoro, L. Marris, C. J. Akerman, and G. Hinton, "Backpropagation and the brain," *Nature Reviews Neuroscience*, pp. 1–12, 2020.
- [13] A. H. Marblestone, G. Wayne, and K. P. Kording, "Toward an integration of deep learning and neuroscience," *Frontiers in Computational Neuroscience*, vol. 10, p. 94, 2016.
- [14] R. C. O'Reilly, "Biologically plausible error-driven learning using local activation differences: The generalized recirculation algorithm," *Neural computation*, vol. 8, no. 5, pp. 895–938, 1996.
- [15] R. J. Prill, P. A. Iglesias, and A. Levchenko, "Dynamic properties of network motifs contribute to biological network organization," *PLoS Biol*, vol. 3, no. 11, p. e343, 2005. [Online]. Available: <http://www.ncbi.nlm.nih.gov/pubmed/16187794>
- [16] A. Tavanaei, M. Ghodrati, S. R. Kheradpisheh, e. Masquelier, Timoth  , and A. Maida, "Deep learning in spiking neural networks," *Neural Networks*, 2018.
- [17] S. Wo  niak, A. Pantazi, T. Bohnstingl, and E. Eleftheriou, "Deep learning incorporating biologically inspired neural dynamics and in-memory computing," *Nature Machine Intelligence*, vol. 2, no. 6, pp. 325–336, 2020.
- [18] Z.-H. Zhou and J. Feng, "Deep forest: Towards an alternative to deep neural networks," *arXiv preprint arXiv:1702.08835*, 2017.
- [19] W. Maass, "Networks of spiking neurons: the third generation of neural network models," *Neural Networks*, vol. 10, no. 9, pp. 1659–1671, 1997.
- [20] Y. Bengio, T. Mesnard, A. Fischer, S. Zhang, and Y. Wu, "Sdp as presynaptic activity times rate of change of postsynaptic activity approximates back-propagation," *Neural Computation*, vol. 10, 2017.
- [21] G. Bi and M. Poo, "Synaptic modifications in cultured hippocampal neurons: Dependence on spike timing, synaptic strength, and postsynaptic cell type," *The Journal of Neuroscience*, vol. 18, no. 24, pp. 10464–10472, 1998.
- [22] R. S. Zucker, "Short-term synaptic plasticity," *Annual Review of Neuroscience*, vol. 12, no. 1, pp. 13–31, 1989.
- [23] T. J. Teyler and P. DiScenna, "Long-term potentiation," *Annual Review of Neuroscience*, vol. 10, no. 1, pp. 131–161, 1987.
- [24] M. Ito, "Long-term depression," *Annual Review of Neuroscience*, vol. 12, no. 1, pp. 85–102, 1989.
- [25] L. F. Abbott and S. B. Nelson, "Synaptic plasticity: taming the beast," *Nature Neuroscience*, vol. 3, no. 11s, p. 1178, 2000.
- [26] C. Blakemore and E. A. Tobin, "Lateral inhibition between orientation detectors in the cat's visual cortex," *Experimental Brain Research*, vol. 15, no. 4, pp. 439–440, 1972.
- [27] G.-q. Bi and M.-m. Poo, "Synaptic modification by correlated activity: Hebb's postulate revisited," *Annual review of neuroscience*, vol. 24, no. 1, pp. 139–166, 2001.
- [28] E. J. Nestler and W. A. Carlezon, "The mesolimbic dopamine reward circuit in depression," *Biological Psychiatry*, vol. 59, no. 12, pp. 1151–1159, 2006.
- [29] C. Frenkel, M. Lefebvre, and D. Bol, "Learning without feedback: Direct random target projection as a feedback-alignment algorithm with layerwise feedforward training," *arXiv: Machine Learning*, 2019.
- [30] D. Zhao, Y. Zeng, T. Zhang, M. Shi, and F. Zhao, "Glsnn: A multi-layer spiking neural network based on global feedback alignment and local stdp plasticity," *Frontiers in Computational Neuroscience*, vol. 14, p. 101, 2020.
- [31] M. Luko  evi  ius, H. Jaeger, and B. Schrauwen, "Reservoir computing trends," *KI-K  nstliche Intelligenz*, vol. 26, no. 4, pp. 365–371, 2012.
- [32] J. P. Wolfgang Maass, "Special issue on echo state networks and liquid state machines," *Neural Networks*, 2007.
- [33] E. M. Izhikevich, "Simple model of spiking neurons," *IEEE Transactions on Neural Networks*, vol. 14, no. 6, pp. 1569–1572, 2003.
- [34] M. Zhang, H. Qu, X. Xie, and J. Kurths, "Supervised learning in spiking neural networks with noise-threshold," *Neurocomputing*, vol. 219, pp. 333–349, 2017.
- [35] L. F. Abbott, B. DePasquale, and R.-M. Memmesheimer, "Building functional networks of spiking model neurons," *Nature Neuroscience*, vol. 19, no. 3, p. 350, 2016.
- [36] Y. Cao, Y. Chen, and D. Khosla, "Spiking deep convolutional neural networks for energy-efficient object recognition," *International Journal of Computer Vision*, vol. 113, no. 1, pp. 54–66, 2015.
- [37] M. Matsugu, K. Mori, M. Ishii, and Y. Mitarai, "Convolutional spiking neural network model for robust face detection," *Iconip'02: Proceedings of the 9th International Conference on Neural Information Processing*, pp. 660–664, 2002. [Online]. Available: [GotoISI://WOS:000182832400136](http://www.gotolibrary.org/WOS:000182832400136)
- [38] E. Rueckert, D. Kappel, D. Tanneberg, D. Pecevski, and J. Peters, "Recurrent spiking networks solve planning tasks," *Scientific reports*, vol. 6, p. 21142, 2016.
- [39] F. Zenke, E. J. Agnes, and W. Gerstner, "Diverse synaptic plasticity mechanisms orchestrated to form and retrieve memories in spiking neural networks," *Nature communications*, vol. 6, 2015.
- [40] F. Ponulak, "Analysis of the resume learning process for spiking neural networks," *International Journal of Applied Mathematics and Computer Science*, vol. 18, no. 2, pp. 117–127, 2008.
- [41] S. M. Bohte, J. N. Kok, and J. A. Poutre, "Spikeprop: backpropagation for networks of spiking neurons," in *the european symposium on artificial neural networks*, 2000, Conference Proceedings, pp. 419–424.
- [42] J. H. Lee, T. Delbruck, and M. Pfeiffer, "Training deep spiking neural networks using backpropagation," *Frontiers in Neuroscience*, vol. 10, 2016.
- [43] G. Bellec, F. Scherr, E. Hajek, D. Salaj, R. Legenstein, and W. Maass, "Biologically inspired alternatives to backpropagation through time for learning in recurrent neural nets," *arXiv preprint arXiv:1901.09049*, 2019.
- [44] Y. Wu, L. Deng, G. Li, J. Zhu, and L. Shi, "Spatio-temporal backpropagation for training high-performance spiking neural networks," *Frontiers in neuroscience*, vol. 12, 2018.
- [45] F. Zenke and S. Ganguli, "Superspike: Supervised learning in multilayer spiking neural networks," *Neural computation*, vol. 30, no. 6, pp. 1514–1541, 2018.
- [46] A. Tavanaei and A. Maida, "Bp-stdp: Approximating backpropagation using spike timing dependent plasticity," *Neurocomputing*, vol. 330, pp. 39–47, 2019.
- [47] Y. Dan and M.-m. Poo, "Spike timing-dependent plasticity of neural circuits," *Neuron*, vol. 44, no. 1, pp. 23–30, 2004.
- [48] P. U. Diehl and M. Cook, "Unsupervised learning of digit recognition using spike-timing-dependent plasticity," *Frontiers in Computational Neuroscience*, vol. 9, 2015. [Online]. Available: [GotoISI://WOS:000360180400001](http://www.gotolibrary.org/WOS:000360180400001)
- [49] S. R. Kheradpisheh, M. Ganjtabesh, S. J. Thorpe, and e. Masquelier, Timoth  , "Sdp-based spiking deep convolutional neural networks for object recognition," *Neural Networks*, vol. 99, pp. 56–67, 2018.
- [50] M. Mozafari, M. Ganjtabesh, A. Nowzari-Dalini, S. J. Thorpe, and e. Masquelier, Timoth  , "Bio-inspired digit recognition using reward-modulated spike-timing-dependent plasticity in deep convolutional networks," *Pattern Recognition*, vol. 94, pp. 87–95, 2019.
- [51] T. Zhang, Y. Zeng, M. Shi, and D. Zhao, "A plasticity-centric approach to train the non-differential spiking neural networks," in *Thirty-Second AAAI Conference on Artificial Intelligence*, 2018, Conference Proceedings, pp. 620–628.
- [52] B. Scellier and Y. Bengio, "Equilibrium propagation: Bridging the gap between energy-based models and backpropagation," *Frontiers in Computational Neuroscience*, vol. 11, pp. 24–24, 2017.
- [53] T. Zhang, Y. Zeng, D. Zhao, and B. Xu, "Brain-inspired balanced tuning for spiking neural networks," in *International Joint Conference on Artificial Intelligence*, 2018, Conference Proceedings, pp. 1653–1659.
- [54] Y. Zeng, T. Zhang, and B. Xu, "Improving multi-layer spiking neural networks by incorporating brain-inspired rules," *Science China Information Sciences*, vol. 60, no. 5, p. 052201, 2017.
- [55] T. Zhang, Y. Zeng, D. Zhao, L. Wang, Y. Zhao, and B. Xu, "Hm-snn: Hippocampus inspired memory spiking neural network," in *IEEE International Conference on Systems, Man and Cybernetics*, 2016, Conference Proceedings, pp. 002 301–002 306.
- [56] M. Shi, T. Zhang, and Y. Zeng, "A curiosity-based learning method for spiking neural networks," *Frontiers in Computational Neuroscience*, vol. 14, p. 7, 2020.
- [57] S. M. Bohte, J. N. Kok, and H. La Poutre, "Error-backpropagation in temporally encoded networks of spiking neurons," *Neurocomputing*, vol. 48, no. 1, pp. 17–37, 2002.

- [58] R. M. Fitzsimonds, H. J. Song, and M. M. Poo, "Propagation of activity-dependent synaptic depression in simple neural networks," *Nature*, vol. 388, no. 6641, pp. 439–48, 1997. [Online]. Available: <https://www.ncbi.nlm.nih.gov/pubmed/9242402>
- [59] M. Häusser, N. Spruston, and G. J. Stuart, "Diversity and dynamics of dendritic signaling," *Science*, vol. 290, no. 5492, pp. 739–744, 2000.
- [60] K. Svoboda, F. Helmchen, W. Denk, and D. W. Tank, "Spread of dendritic excitation in layer 2/3 pyramidal neurons in rat barrel cortex in vivo," *Nature Neuroscience*, vol. 2, no. 1, pp. 65–73, 1999.
- [61] A. Paszke, S. Gross, S. Chintala, G. Chanan, E. Yang, Z. DeVito, Z. Lin, A. Desmaison, L. Antiga, and A. Lerer, "Automatic differentiation in pytorch," in *NIPS-W*, 2017.
- [62] Y. LeCun, "The mnist database of handwritten digits," <http://yann.lecun.com/exdb/mnist/>, 1998.
- [63] A. Krizhevsky and G. Hinton, "Learning multiple layers of features from tiny images," *Tech Report*, 2009.
- [64] R. G. Leonard and G. Doddington, "Tidigits ldc93s10," *Web Download. Philadelphia: Linguistic Data Consortium*, 1993.
- [65] A. Amir, B. Taba, D. Berg, T. Melano, J. McKinstry, C. Di Nolfo, T. Nayak, A. Andreopoulos, G. Garreau, and M. Mendoza, "A low power, fully event-based gesture recognition system," in *Proceedings of the IEEE Conference on Computer Vision and Pattern Recognition*, Conference Proceedings, pp. 7243–7252.
- [66] P. U. Diehl, D. Neil, J. Binas, M. Cook, S.-C. Liu, and M. Pfeiffer, "Fast-classifying, high-accuracy spiking deep networks through weight and threshold balancing," in *Proceedings of the 2015 International Joint Conference on Neural Networks*. IEEE, 2015, pp. 1–8.
- [67] J. Wu, Y. Chua, M. Zhang, H. Li, and K. C. Tan, "A spiking neural network framework for robust sound classification," *Frontiers in Neuroscience*, vol. 12, 2018.
- [68] Y. Zhang, P. Li, Y. Jin, and Y. Choe, "A digital liquid state machine with biologically inspired learning and its application to speech recognition," *IEEE Transactions on Neural Networks*, vol. 26, no. 11, pp. 2635–2649, 2015.
- [69] M. E. Davies, N. Srinivasa, T. Lin, G. Chinya, Y. Cao, S. H. Choday, G. D. Dimou, P. Joshi, N. Imam, S. Jain *et al.*, "Loihi: A neuromorphic manycore processor with on-chip learning," *IEEE Micro*, vol. 38, no. 1, pp. 82–99, 2018.



Tielin Zhang received the Ph.D. degree from the Institute of Automation Chinese Academy of Sciences, Beijing, China, in 2016. He is an Associate Professor in the Research Center for Brain-Inspired Intelligence, Institute of Automation, Chinese Academy of Sciences, Beijing, China. His current interests include theoretical research on neural dynamics and Spiking Neural Networks.



Shuncheng Jia is a Ph.D. candidate in both the Institute of Automation Chinese Academy of Sciences and the University of Chinese Academy of Sciences. His current interests include theoretical research on neural dynamics, auditory signal processing, and Spiking Neural Networks.



Bo Xu is a professor, president of the Institute of Automation, Chinese Academy of Sciences, and also deputy director of the Center for Excellence in Brain Science and Intelligence Technology, Chinese Academy of Sciences. His main research interests include brain-inspired intelligence, brain-inspired cognitive models, natural language processing and understanding, brain-inspired robotics.